Asian Journal of Pharmaceutical Sciences 15 (2020) 1–12

Available online at www.sciencedirect.com

ScienceDirect

journal homepage: www.elsevier.com/locate/AJPS

Review

Current multifunctional albumin-based nanoplatforms for cancer multi-mode therapy

Chang Li[a], *Xin Wang*[a], *Hang Song*[b], *Shuai Deng*[a], *Wei Li*[c], *Jing Li*[d,*], *Jin Sun*[a,*]

[a] *Wuya College of Innovation, Shenyang Pharmaceutical University, Shenyang 110016, China*
[b] *College of Pharmacy, Shenyang Pharmaceutical University, Shenyang 110016, China*
[c] *Department of Pharmaceutical Engineering, Shenyang University of Chemical Technology, Shenyang 110142, China*
[d] *School of Basic Medical Science, Shenyang Medical College, Shenyang 110034, China*

ARTICLE INFO

Article history:
Received 7 July 2018
Revised 16 December 2018
Accepted 26 December 2018
Available online 1 March 2019

Keywords:
Albumin
Formulations
Multi-mode therapy
Combination therapy
Stimuli-responsive release

ABSTRACT

Albumin has been widely applied for rational design of drug delivery complexes as natural carriers in cancer therapy due to its distinct advantages of biocompatibility, abundance, low toxicity and versatile property. Hence, various types of multifunctional albumin-based nanoplatforms (MAlb-NPs) that adopt multiple imaging and therapeutic techniques have been developed for cancer diagnosis and treatment. Stimuli-responsive release, including reduction-sensitive, pH-responsive, concentration-dependent and photodynamic-triggered, is important to achieve low-toxicity cancer therapy. Several types of imaging techniques can synergistically improve the effectiveness of cancer therapy. Therefore, combinational theranostic is considered to be a prospective strategy to improve treatment efficiency, minimize side effects and reduce drug resistance, which has received tremendous attentions in recent years. In this review, we highlight several stimuli-responsive albumin nanoplatforms for combinational theranostic.

1. Introduction

Albumin, belonging to the most abundant serum protein (35–50 g/l human serum), is a highly soluble and stable protein. It is responsible for osmotic pressure regulation and transport of fatty acids, drugs, metals and hormones. There are different types of albumin depending on its origin, nevertheless, the well-studied and commonly used albumins are human serum albumin (HSA) and bovine serum albumin (BSA) [1]. HSA molecules also bind many therapeutic drugs and control their *in vivo* fate. HSA with the molecule weight equal to 66 439 Da consists of 585 amino acids [2]. Its crystalline structure consists of 69% a-helix [3]. In aqueous solution, HSA molecule exhibits positive electrophoretic mobility at pH < 5 due to cysteine, tyrosine, arginine and lysine amino acid esidues, and

* Corresponding authors: Wuya College of Innovation, Shenyang Pharmaceutical University, Shenyang 110016, China. Tel.: +86 24 23986325.
E-mail addresses: dddefghijklmn@163.com (J. Li), sunjin@syphu.edu.cn (J. Sun).
Peer review under responsibility of Shenyang Pharmaceutical University.

https://doi.org/10.1016/j.ajps.2018.12.006

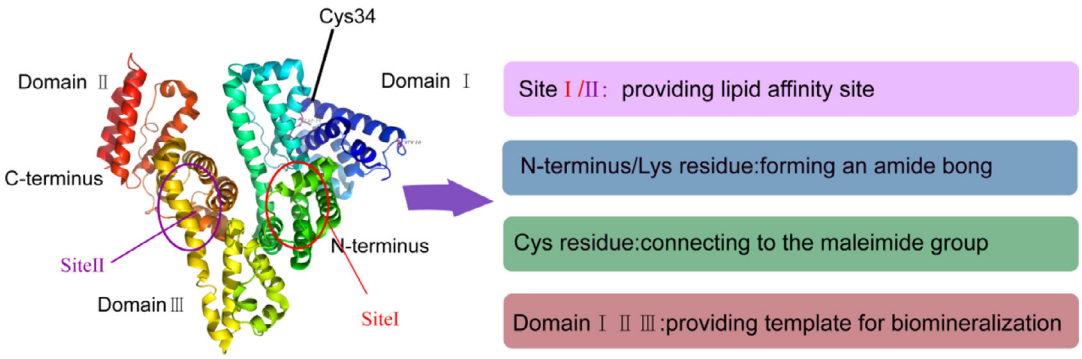

Fig. 1 – Modular domain structure and functionof the HSA molecule.

its isoelectric point is equal to *ca*. 5.1.As shown in Fig. 1, the shape of HSA molecule is irregular characterized by no symmetry axis resembling a heart shape [4], which corresponds to the N-form of albumin [1,5]. Generally, albumin is a perfect nanocarrier for drug delivery due to its natural structural roles, innocuous degradation metabolites, water solubility, availability of pure forms and full biocompatibility. Albumin has a long half-life of 19 days in blood, and can preferentially accumulate in tumor because tumor cells actively metabolize albumin to meet their increased demand for amino acids and energy.

The design of a drug delivery system typically uses specific ligands for tumor targeting. However, less than 5% of the intravenously injected dosage can reach tumor site. Smart nanocarriers that are sensitive to exogenous or endogenous stimuli represent another targeted drug delivery method [6]. Due to its specific environment- responsive characteristics, it is possible to achieve a specific dose of on-demand drug release at a specific site and in a specific time. The principle is that drug release was achieved by using the endogenous and exogenous stimulation to make the drug carrier produce physical or chemical changes. In recent years, the diversity of responsive materials has been assembled indifferent architectures, allowing great flexibility in designing stimulus-responsive systems on-demand. Albumin shows high affinity with gp60 and secreted protein acidic and rich in cysteine (SPARC) that is over expressed on tumor cell surfaces. Amino acids were reported as a source of energy for fast-growing cancer cells. Thereby, albumin could be used for tumor targeting [7]. Besides, stimuli-responsive drug delivery can effectively improve the specific uptake and tissue distribution of the drug, therefore, it also be applied in a targeted drug delivery strategy in MAlb-NPs [6].

Recently, the albumin-based nanoplatforms in cancer multi-mode therapy have achieved tremendous progresses. Common clinical cancer treatment methods, including surgical resection, chemotherapy and radiation therapy, exhibit a relative high toxic profile with a narrow therapeutic window, leading to limited therapeutic efficacy and toxic side effects [8]. Despite great efforts in the past decades, the state of cancer therapy is still not satisfactory until the emergence of a combination therapy [9]. In all types of combination therapies, combing phototherapy and chemotherapy, in which drug and nanoscale theranostic agents could be delivered simultaneously, has attracted increasing interest for clinical cancer treatments. Phototherapy, including photodynamic therapy (PDT) and photothermal therapy (PTT), provides a novel and noninvasive photothermal and photodynamic (PDT+PTT) [10].

Multi-mode therapy, which relies on chemotherapy, radiotherapy, hyperthermia and other monotherapy, cooperates with imaging technology to achieve the diagnosis and integrated treatment [11]. Several types of biomedical imaging techniques were used as an aid in guiding cancer phototherapy, such as magnetic resonance imaging (MRI), fluorescence imaging (FLI), photoacoustic imaging (PAI) and computed tomography (CT). MRI, which allows for whole body imaging, is a diagnostic imaging model extensively used for clinical diagnosis and prognosis of cancer due to its capability to provide three dimensional topographical data with high spatial resolution [12,13]. FLI has ability to monitor the *in vivo* dynamic distribution of photosensitizer or photothermal agent in real time. Moreover, it can detect the normal tissue, tumor and its edges using contrast enhancement and spectral resolution techniques. PAT has high spatial resolution for optical imaging and high penetration depth for ultrasound imaging. It can produce multi-scale multi-contrast images of living organisms from organelles to organs, thus overcoming some of the limitations of NIR FL imaging [14]. X-ray CT imaging is one of the most commonly used imaging tools for clinic diagnosis and medical research. It utilizes difference in the absorption effect from different human tissues to produce images for body structures and tissues [15]. Contrast agents (*e.g.* iodine, gold, bismuth, tantalum and lanthanides), higher or lower density compared to the target structure or organ, are introduced into the organ or its surrounding gaps to absorb and weaken the incident X-rays to produce tissue contrasts in the diagnostic regime [16,17]. The comparison of various imaging modalities in preclinical application is summarized in Table 1.

Herein, we will mainly report the recent progresses in the past five years, regarding the development of MAlb-NPs.

Table 1 – Comparison of various imaging modalities in preclinical use.

	MRI	OPI	PAT	CT
Detection sources	• magnetic, • field, • radiowaves	• visible or near-infrared light	• short-pulsed laser beam	• X-ray
Advantages	• applicable for human, • high spatial resolution, • no tissue penetrating limit	• inexpensive • easy operation	• high resolution and contrast	• anatomical imaging, • applicable for humans
Disadvantages	• scan and processing, • relatively low sensitivity, • time and money consuming	• photobleaching, • surface-weighted, • autofluorescence disturbance, • relatively low spatial resolution • limited tissue penetrating depth	• high frequency or photoacoustic signals	• radiation risks, • not quantitative, • limit soft tissue resolution
Applications	• cell trafficking, • gene expression, • morphological reporter, • cerebral and coronary angiography in clinics	• trafficking or movement monitoring of reporter/gene, • cellular/intracellular expression	• endoscopy, • gene expression, • molecular imaging, • melanoma detection	• bone and tumor imaging, • fused image with other modalities

2. The interaction between carrier and cargo in albumin-based nanoplatforms

Albumin is synthesized and secreted by the liver, and it circulates in the blood and the larger organs of human body. As carriers, some hydrophobic molecules are positively charged molecules or particles can be bound to albumin. And as nutrients, it is digested and decomposed by cells, providing amino acids for cell metabolism. Albumin is widely applied to pharmaceutical preparations study as a carrier for drug delivery based on its mimicking nutrient transport mechanism [18].

Albumin has attracted broad attention owing to its inherent biocompatibility and extraordinary binding capacity for loading a wide variety of drug molecules. There are two main drug loading methods. The first one is to create the molecular linker between drug and albumin carrier to form an albuminized drug, which belongs to the chemically conjugated albumin drug delivery method. The other one is to rely on the interaction between protein and drug to entrap the drug in albumin nanoparticles, which is physically bound albumin drug delivery method. Chemically conjugated albumin can improve the pharmacokinetic properties of drugs, which can be further divided into exogenous albumin and drug coupling, prodrugs into the body to bind with endogenous albumin, the albuminized of protein or peptide drugs. Physically bound albumin is capable of optimizing *in vitro* characteristics (solubility, stability) of the drug. Especially in the last few decades, the rational design of albumin-based nanoplatforms has become a focused research in the fields of pharmaceutics. In this paper, we review various types of MAlb-NPs, which are strategically functionalised by cargo to achieve multiple imaging and therapies for cancer.

All kinds of cargoes (drugs, dye, photosensitizer) can be incorporated with albumin *via* biomineralization, covalent conjugationor hydrophobic interaction [5]. The examples of forming method or function between albumin and various cargoes are summarized in Table 2.

2.1. *The cargo binds albumin through hydrophobic interactions*

Since the structure of albumin with hydrophobic, hydrophilic domains and abundant charged amino acids, it is able to load multifarious cargoes with different physicochemical properties without the need of other compounds. Indocyanine green (ICG) is a clinically used near-infrared (NIR) dye that has been approved by the US FDA for both fluorescence imaging and PTT. ICG can be adsorbed onto the hydrophobic domain of each HSA by hydrophobic binding [19]. For example, Chen et al. found that though ICG could be adsorbed onto the hydrophobic domain of each HSA, the formed complex may not be as stable as the complex formed between HSA and PTX [20]. Therefore, PTX with a much higher hydrophobicity upon binding to HSA, could act as an “adhesive” between different albumin and induce assembly of many albumins to establish large nanoparticles with the entrapment of both ICG and PTX. PTX induced assembly of HSA and could enhance the stability of ICG loading in the formed nanoparticles. What’s more, the combination with HSA improved the fluorescence emission of ICG.

Similarly, DHA-paclitaxel prodrugs delivered drug by binding to the lipophilic binding site of albumin (Fig. 2A).

2.2. *Covalent binding of cargo and albumin*

Each albumin molecule contains not only 59 amino acid residues and one N-terminal carboxyl group for drug attachment, but also Cys-34 residues that can participate in the reaction. There are two ways to use the albumin amino acid residues to covalently link the cargo directly or *via* linker. One

Table 2 – Typical example of albumin-carried cargoes.

Theranostics agents species		Type of cargoes	Forming method/function	References
Diagnostic agents	MRI	Gd^{3+}	chelation	[44]
		Mn^{2+}	chelation	[45]
		Iron oxide	contrast agents	[46]
	CT	^{125}I	contrast agent	[47]
		Au	contrast agent	[48]
	OPI	Quantum dots	conjugate	[49]
		FLI	–	[39]
	PAI	Au nanostructures	–	[50]
		Croconine	self-assembly	[51]
	PET	^{64}Cu	label	[52]
		^{68}Ga	label	[53]
Therapeutic agents	ChT	DOX	conjugate/crosslink	[54]/[55]
		paclitaxel	self-assembly	[56]
	RIT	Au	biomineralization	[25]
	PDT	ICG	Hydrophobic interaction/intermolecular disulfide conjugation	[20]
		Ce6	covalent conjugation	[34]
		Pheophorbide a	conjugation	[57]
	PTT	Au nanostructures	–	[58]
	Radioisotope Therapy	^{131}I	label	[30]

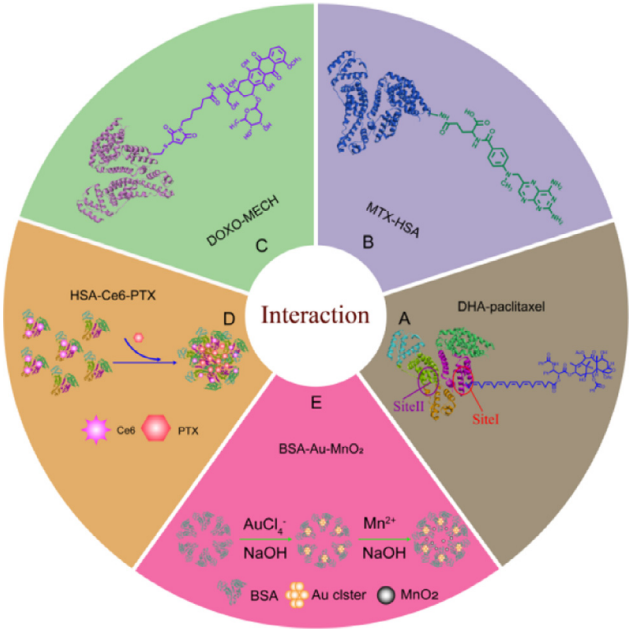

Fig. 2 – A schematic illustration of interaction betweenalbumin andcargos in albumin-based nanoplatforms.

is to apply lysine residues to form an amide bond, and the other is to attach cysteine residues to a maleimide group.

For example, Burger et al. conjugated methotrexate (MTX) to HSA with an amide binding preferably *via* the γ-carboxyl group of a free lysine rest in HSA [21] (Fig. 2B). Interestingly, they found that the drug conjugates bearing multiple MTX molecules per albumin were rapidly cleared from circulation and predominately trapped by the monocyte–macrophage system of the liver. However, albumin conjugated with MTX at an equimolar drug-carrier ratio (1:1) exerted a higher tumor-targeting effect. Chlorin e6 (Ce6), a clinically used photodynamic reagent that conjugated to HSA through forming an amide bond. In another study, Mocanu et al. reported that Ce6 can be strongly bound to HSA at or near physiological pH conditions (Fig. 2D), but the strength of the binding is significantly weakened at lower pH [22].

Connecting a drug to a linker with a maleimide group and attaching it to the Cys-34 residue of albumin either *in vivo* or *in vitro* also enable the covalently attachment of protein and cargo. For instance, Kratz et al. connected Doxorubicin to linker (Maleimides, etc.) through hydrazone bond, thus forming hydrazone derivative of doxorubicin that bound preferentially and rapidly to cysteine-34 of endogenous albumin. It had superior antitumor efficacy in murine renal cell carcinoma compared to doxorubicin [23] (Fig. 2C).

2.3. *The cargo is bound to albumin by biomineralization*

Biomineralization is the process that organisms generate inorganic minerals through the regulation of biological macromolecules. Biomineralization has the effect of converting ions in solution into solid minerals under certain physical and chemical conditions and under the control or influence of biological organic matter. According to the report, albumin could be used as a template to chelate and interact with inorganic ions under alkaline conditions through biomineralization to form protein-coated minerals [24]. In recent years, a convenient biomineralization method was proposed to fabricate MAlb-NPs containing biocompatible/biodegradable ingredients for enhanced cancer therapy. For example, Chen et al. used BSA as a template to induce the growth of both gold (Au) nanoclusters and manganese dioxide (MnO_2) *via* biomineralization with the optimized feeding molar ratio

of BSA: manganese chloride ($MnCl_2$) (1:40) [25]. Within the obtained BSA-Au-MnO_2 composite nanoparticles (Fig. 2E), Au nanoclusters embedded in BSA showed a strong red fluorescence to promote imaging, and served as a radio-sensitizer by absorbing the x ray energy within the tumor to enhance radiation therapy. In addition, the MnO_2 core was able to decompose into O_2 in acidic tumor microenvironment to resolve tumor hypoxia, thereby reversing the hypoxia-related radiation resistance of tumors.

3. Stimuli-response of MAlb-NPs

In addition, in order to further enhance the therapeutic effect, an albumin-based intelligent multifunctional nanoplatform is designed as stimuli-responsive nanosystem. It responds to internal or external triggers, changing from the intrinsic physiological-microenvironmental (pH, redox, reactive oxygen species (ROS), Concentrations, enzymes, heat, etc.) and/or external artificially introduced triggers (light, magnetic/electric fields, ultrasound, etc.) for on-demand drug release [26,27].

3.1. *Endogenous stimulation*

3.1.1. *pH-sensitive MAlb-NPs*

According to published literature, inflamed tissues and tumor tissues uptake excessive nutrient and lack of dissolved oxygen. Since an aerobic respiration produced more acidic substances (weak acids and CO_2), their pH was much lower than that in blood and normal tissue [28]. Nanoparticles loaded drugs in a mild acidic environment can be used for a wide range of applications by releasing the loaded cargo for drug release from internal pH [26]. It is known that the nanoparticle size usually plays a crucial role in controlling their retention and penetration in tumor. However, the tumor-associated fibroblasts and dense extracellular matrix will be the major barrier for the deep interstitial penetration of nanoparticles with large size. On the other hand, nanoparticles with sizes below 10 nm are characterized with better intratumoral penetrating efficiency but possibly reduced EPR (enhanced permeability and retention) effect. Thus, it has been proposed that ideal nanomedicine particles should be relatively large (50–100 nm) during blood circulation to achieve effective EPR tumor accumulation, but once inside the tumor, they ought to be small enough for enhanced penetration. This phenomenon has stimulated the exploration and research of a large number of MAlb-NPs based on response to physiologic pathological pH changes to selective trigger drug release in tumor microenvironment (TME) and increase deep penetration of tumors.

Liu group [29] developed multifunctional intelligent pH-H_2O_2-responsive HSA-MnO_2–Ce6&Pt(HMCP) nanoparticles or effective combination therapy. The design mechanism is as follows. HSA was first preconjugated with either Ce6 or cis-Pt(IV)SA *via* the formation of amide bond to yield individualHSA-Ce6 (HC) or HSA-Pt(IV) (HP) albumin-drug complexes with sizes below 10 nm. Then HC and HP dispersed in water were mixed with $MnCl_2$ under vigorous stirring. Manganese ion (Mn^{2+}) would be anchored to the active groups such as carboxyl groups and thiol groups of HSA to form albumin-Mn complexes. Meanwhile, NaOH was used to adjust the pH value of the mixture and trigger the following reaction:

$$2MnCl_2 + 4NaOH + O_2 \rightarrow MnO_2 + 4NaCl + 4H_2O.$$

HMCP nanoparticles with sizes of ~50 nm showed potent tumor accumulation by the EPR effect. Once inside the tumor, MnO_2 nanoclusters within HMCP nanoparticles could overcome the hypoxia-associated PDT resistance by triggering the tumor's endogenous H_2O_2 decomposition into oxygen to regulate tumor hypoxia. In the meanwhile, HMCP nanoparticles would degrade into individual HSA-Ce6 or HSA-Pt(IV) albumin-drug complexes with small sizes less than 10 nm, once inside the acidic TME with reduced pH to allow deep interstitial diffusion (Fig. 3), which could be explained by the following reactions.

$$MnO_2 + 2H^+ \rightarrow Mn^{2+} + H_2O + 1/2O_2\uparrow,$$

$$MnO_2 + H_2O_2 + 2H^+ \rightarrow Mn^{2+} + 2H_2O + O_2\uparrow.$$

In another study conducted by Tian et al., radionuclide ^{131}I labeled HSA-bound manganese dioxide nanoparticles (^{131}I-HSA-MnO_2) were designed as a novel radioisotope therapy (RIT) nanoplatform that was responsive to the TME. In such ^{131}I-HSA-MnO_2 nanoparticles, iodine-131 emitting β and γ rays could be used for RIT and nuclear imaging. The design mechanism is similar to the above HMCP nanoparticles. In brief, HSA solution was first mixed with $MnCl_2$in alkaline to form HSA-MnO_2 nanoparticles through a biomineralization process. Then, the obtained HSA-MnO_2 nanoparticles were labeled with iodine-131, a clinically used radioisotope, thus yielding ^{131}I-HSA-MnO_2. HSA was a biocompatible natural nanocarrier for efficient radionuclide labeling and delivery, and it served as the nano template to induce the growth of MnO_2. After entering the tumor micro environment with reduced pH through the EPR, ^{131}I-HSA-MnO_2 nanoparticles with the acid-triggered decomposition of MnO_2 would be degraded into individual radiolabeled HSA with enhanced intratumoral diffusion (Fig. 4), resulting inenhanced intra-tumoral permeability [30].

3.1.2. *Reductive-sensitive MAlb-NPs*

Some substances with reductive properties show high expression in tumor tissue microenvironment, such as glutathione (GSH) and dithiothreitol. According to reports, the concentration of these substances in tumor tissue microenvironment of mice is at least 4 times higher than that in normal tissues. At the same time, there is often a large difference in GSH concentration between the intracellular and extracellular environment, which is approximately 2–10 mM in cells, but it is as low as approximately 2–20 μM in the extracellular environment.

Disulfide bonds have attracted more and more attention in nanodrug delivery systems with reduced response [31]. Since each HSA molecule consists of one sulfhydryl group and 17 pairs of disulfide bonds. Sheng et al. prepared HSA-ICG nanoparticles (HSA-ICG NPs) *via* reducing the intramolecular disulfide bonds of HSA by GSH and the resulting free

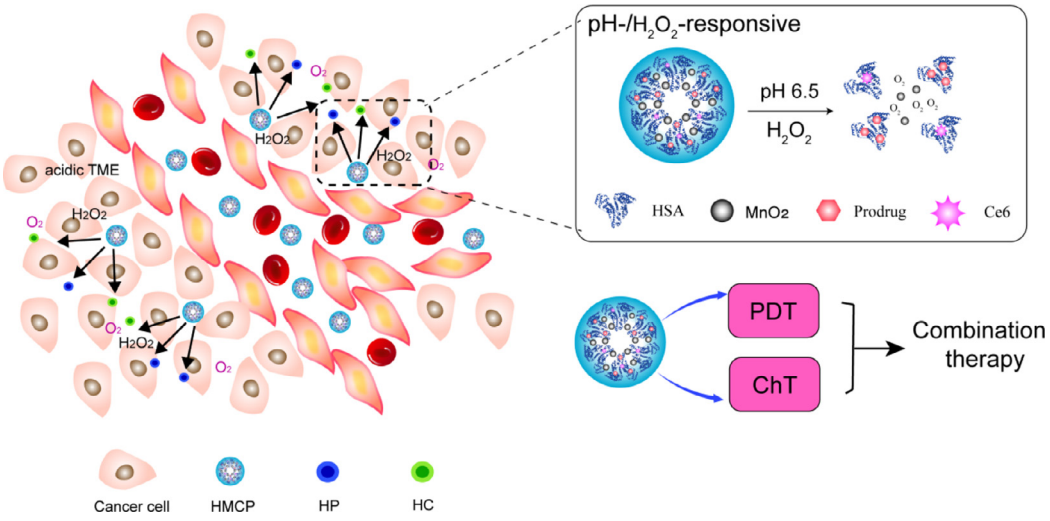

Fig. 3 – A schematic illustrating the pH-sensitive release and dissociation process of HCMP in the tumor micro environment to allow deep interstitial penetration of therapeutic albumin complexes (HC and HP).

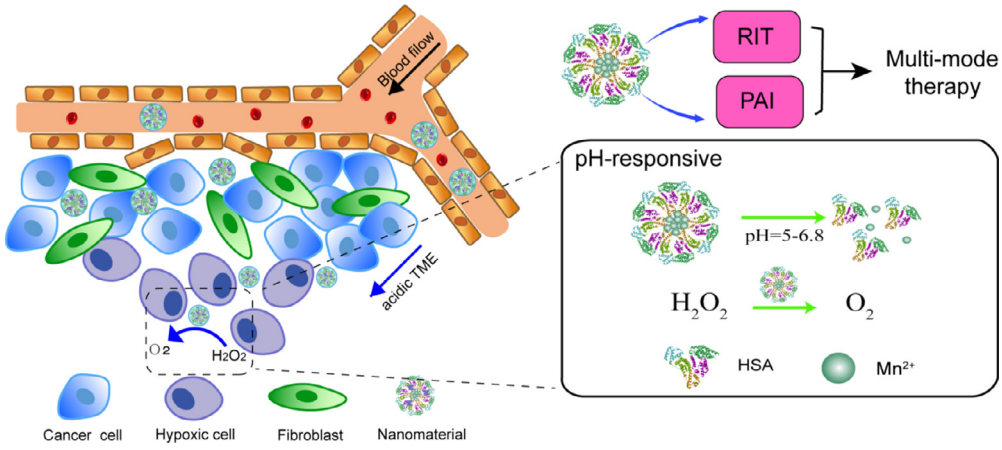

Fig. 4 – A schematic illustration to show the pH-sensitive release process of ^{131}I-HSA-MnO$_2$.

sulfhydryl groups were reassembled by intermolecular disulfide bonds and then HSA NPs were formed. In this study, the HSA was incubated with excessive glutathione (GSH), an endogenous reducing agent, and these disulfide bonds of HSA molecular were cleaved. The obtained free sulfhydryl groups were assembled again by intermolecular disulfide bonds and formed HSA NP. The formations of intermolecular disulfide bonds are prone to stabilize the HSA-ICG NPs and make the NPs have reductive-sensitive activity. *In vivo*, the encapsulation of ICG in HSA NPs prevents its interaction with the surrounding environment and delays its decomposition, thereby improving the photothermal and colloidal stability as well as biocompatibility of ICG (Fig. 5A). HSA-ICG NPs not only possess passive and active tumor-targeting capabilities *via* EPR effect, gp60 and SPARC receptor-mediated transcytosis, but also exhibit excellent reductive-sensitive activity [32].

3.1.3. *Concentration-dependent response of MAlb-NPs*

As mentioned above, the complex composition and structure of tumor leads to an increase in compressed tumor blood vessels and interstitial fluid pressure, which can seriously affect the penetration of therapeutic drugs, especially during the treatment of cancer with relatively large size nanoparticles. Thus, MAlb NPs with variable size can maintain a relatively large size (50–100 nm) during blood circulation and effectively accumulate tumors through EPR effects. Separating into small particles within the tumor (less than 10 nm) would be very important for deeper penetration [33].

Chen et al. confirmed that HSA-Ce6-Cat-PTX NPs (one type of MAlb-NPs) was fabricated by inducing co-assembly of catalase and HSA utilizing PTX, the latter of which was pre-modified with Ce6. Their stability comparison was made by drug induced self-assembly with chemical cross-linking. The PTX-induced HSA-Ce6-Cat-PTX self-assembly is non-covalent, but the addition of glutaraldehyde cross-linking agent formed HSA-Ce6-Cat NPs that relies on covalent forces. Therefore, some of the non-public valence forces of HSA-Ce6-Cat-PTX nanoparticles are easily destroyed when the external concentration changes. The measured hydrodynamic diameters indicated that HSA-Ce6-Cat-PTX would gradually

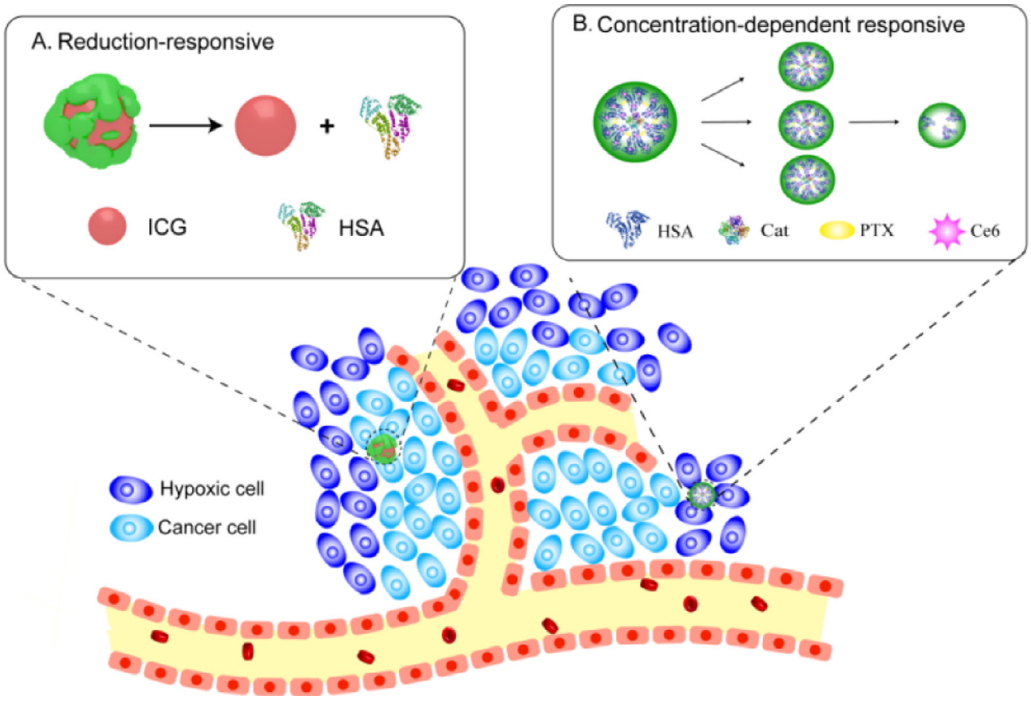

Fig. 5 – The examples of reduction-sensitive of (A) HSA-ICG and concentration-dependent response of (B) HSA-Ce6-Cat-PTX.

dissociate upon dilution, while HSA-Ce6-Cat NPs obtained by chemical cross-linking were quite stable at different concentrations. Chemically cross-linked albumin nanoparticles with large sizes (~100 nm) appear to show excellent passive tumor accumulation by the EPR effect owning to their prolonged blood circulation. However, the tumor-associated fibroblasts and dense extracellular matrix will limit their interstitial penetration within the tumor. On the contrary, HSA-Ce6-Cat-PTX could maintain large initial sizes (~100 nm) during blood circulation then may gradually disintegrated into smaller(<20 nm) therapeutic albumin-drug complexes within the tumor based on their concentration dependent dissociation behavior, leading to a significant increase in intratumoral permeability [34] (Fig. 5B).

3.2. *Exogenous stimulation*

There are still some anti-tumor drug delivery systems with external stimulus triggering release characteristics. These external stimulus include light stimulation, ultrasound stimulation, magnetic field stimulation and thermal stimulation. The important advantages of release control can be divided into precise time and space control, on-demand dose control and non-invasive characteristics with optional switch control.

In such external controls, light radiation stimulation has a great deal of randomness in changing light irradiation intensity and the site of action. This section focuses on the light [35]. Peralta et al. confirmed that photothermal approach treats hyperthermic, and acts as a trigger for drug release once the particles have reached their targeted tissue. In addition, Chen et al. observed that both HSA-Ce6-PTX-rgd-1 and HSA-Ce6-PTX-rgd-2 nanoparticles were identified to lead synergistic cancer killing after being exposed to the 660 nm light irradiation. This phenomenon implied the photodynamic effect induced endosomal/lyosomal degradation and the subsequent endosomal escape, thus improving the therapeutic efficiency of these cargoes [36]. As we know, the control ability of light radiation is crucial for precise therapy. Controllability of light radiation stimulation could be realised by cooperating with imaging technology. For instance, Sheng et al. put forward that under the guidance of NIR FL and PA dual-modal imaging and spectrum-resolved technology, the laser beam could be manipulated very precisely and flexibly, and accurately focused on the whole tumor tissue. When the continuous NIR laser beam was accurately focused on the whole tumor tissue, the growth of 4T1 tumor was completely inhibited with 100% of survival rate on day 50, and there was no tumor recurrence detected [32].

4. MAlb-NPs for cancer multi-mode therapy

Multi-mode imaging-guided combination therapy promises a more accurate diagnosis and higher therapeutic efficiency than single imaging mode or their simple “mechanical” combination.

Combination of PTT/PDT with ChT offers unique advantages over monotherapy alone. PTT usually utilizes NIR light to absorb photosensitizers, thereby damaging tumor cells with laser irradiation by heating. However, both photosensitizers and chemotherapeutic agents lack tumor-targeted accumulation and can be easily eliminated from the body. In addition, most PTT drugs are hydrophobic and their organic solvents have *in vivo* toxicity, which limits their potential for clinical translation [37].

Since each albumin molecule contains 59 amino acid residues and one N-terminal carboxyl group for drug attachment, Cys-34 residues can also participate in the reaction. And the structure of albumin with both hydrophobic and hydrophilic domains makes it easy to load other therapeutic agents during the combination therapy. For example, ICG can be adsorbed onto the hydrophobic domain of each HSA, Ce6 is conjugated to HSA *via* the formation of an amide bond, HSA serves as the template to induce the growth of MnO_2 nanocrystals, etc. Therefore, MAlb-NPs can be rendered as favorable strategy to solve the above problems in the application of combination therapy.

4.1. *Biomedical imaging multi-mode therapy*

Imaging guided PTT/PDT has been widely applied in pharmaceutical research as one of the most challenging strategies for cancer treatment. Imaging with contrast agent allows non-invasive diagnosis of the disease and real-time monitoring of the particle localization to aid in PTT/PDT [13].

Sasidharan et al. proposed the use of polycationic amino acid poly-L-arginine (PLA) to synthesize albumin nanoparticles that avoids toxic glutaraldehyde ascross-linker to form stable nanoparticles. The addition of gold chloride solution in PLA-Alb NPs results incharge reversal of particles (negative to positive due to acidic pH). This would facilitate the attachment of chloroauric acid ions ($AuCl_4^-$) to the cationic surface provided by PLA-Alb NPs. Further, $AuCl_4^-$ that linked to PLA-Alb NPs was reduced to gold atoms by ascorbic acid (the molar ratio of ascorbic acid to $HAuCl_4 > 1.5{:}1$), which acted as a nucleus for further growth. Finally, BGNs was generated by the conjugation of sulfur from thiol groups of GSH molecules to gold nanostructures. It is reported that it has SPR λ_{max} at 800 nm with marked photothermal cytotoxicity on KB cells and superior CT contrastabilit [38].

Nowadays, theranostic magnetic gadolinium (lanthanide ionGd^{3+})-chelated gold nanoparticles have been extensively studied for precise nanomedicine. However, the conventional modification of gold nanoparticles had low Gd^{3+} loading capacity, and easy leakage of Gd^{3+} would lead to undesired toxicity. With these barriers, You et al. utilized BSA to obtain Gd^{3+}-based complex using biomineralization method. The BSA-Gd complex with the advantages of high longitudinal proton relaxivity prolonged imaging time window, excellent biocompatibility and good stability. These nanoplatforms could be well-reasoned suited for simultaneous photothermal effect and MRI/PAI/CT diagnostic imaging. What's more, ICG, a NIR dye exhibiting strong near-infrared fluorescence(NIRF) and PA imaging was integrated into the Au-BSA−Gd nanoparticles for combining PTT and PDT. Gd^{3+} ions mediated gold nanoclusters self-assemble into monodisperse spherical nanoparticles(GNCNs). For the T1-weighted MRI, an obvious increase was observed in both the luminance and signal to noise ratio (SNR) of T1-weighted cellular MRI of GNCNs with the increase of the Gd^{3+} ions concentration. As the Gd concentration increases from 0 to 25 μM, the SNR changes from about 16 to 30 μM. The CT value of cells treated with GNCNs increased from approximately 15 to 35 μM as the Au concentration enhanced from 0 to 500 μM. Therefore, the GNCNs could be used as a multifunctional nanoplatform for NIRF/CT/MRI ofA549 cancer cells. The ICG−Au-BSA−Gd nanoparticles were proven to show several unique superiorities, such as the quad-modal imaging (NIRF/PAI/CT/MRI) and the simultaneous PDT/PTT effect based on Au-BSA−Gd and ICG [39].

The HSA-ICG NPs (prepared by Sheng et al.) that described in 3.1.2 were intermolecularly cross-linked by disulfide bonds and had excellent reduction sensitivity. The tumor, tumor margin and normal tissue could be clearly detected using ICG-based *in vivo* FL and PA dual-modal imaging and spectrum-resolved technology, which was prone to avoid the effect of light scattering and precisely guide cancer phototherapy. Moreover, the simultaneous synergistic PDT/PTT effect induced by HSA-ICG NPs with single NIR laser could adequately convert the NIR laser energy to ROS and local hyperthermia for enhanced PTT. Therefore, this novel MAlb NPs can be a promising strategy for imaging multi-mode cancer PTT, and is expected to have a great potential application in clinical translation.

4.2. *The combination of ChT and PTT*

In PTT, hyperthermia agents absorb light and dissipate the absorbed energy through heat, which causes an increase in temperature in the local environment, resulting in irreversible cell damage.

Peralta et al. [35] reported that chemotherapeutic drug paclitaxel (PAC) could be effectively loaded within the gold nanorod-human serum albumin nanoparticles (AuNR-HSA). They found that PAC loading enhanced as increasing the amount of PAC and HSA in the preparation progress. Furthermore, when AuNRs were present within the particles, there was a 45% increase in PAC loading (PAC-HSA and PAC-AuNR-HSA entrapped an average of 63.3 ± 14 μg and 91.8 ± 9 μg of PAC, respectively). This drug payload increase was attributed to the design of this particular hybrid formulation. The PAC-AuNR-HSA formulated with 30 mg of HSA, 1.5 ml of AuNRs stock and 0.5 mg of PAC sharply increased to 43 °C in about 5 min and continued to heat to 46 °C within 15 min. Under the same condition, the heating of PAC-HSA without AuNRs inside never reach a temperature higher than normal body temperature. The above experiment demonstrated that AuNRs are necessary for causing a large amount of heating of PAC, and cells resistant to PAC will be killed by hyperthermia, thereby significantly reducing the survival rate of drugs or heat-resistant cells and further exerting synergy effect. When photo thermally active material was notheat-activated, PAC-AuNR-HSA still showed more cell death than PAC-HSA and AuNR-HSA. The irradiated PAC-AuNR-HSA caused more cell necrosis than PAC-HSA at three paclitaxel concentrations, with or without irradiation ($P < 0.001$). The combination of ChT and PTT allows cancer cells to be killed by both hyperthermia and localized chemotherapy treatment. Cells with heat-resistance will be killed by chemotherapy [35].

In another report, Chen et al. utilized the formulated HSA-ICG-PTX nanoparticles (the molar ratio of HSA: ICG: PTX = 1:2:10) to effectively combine PTT and ChT under the guidance of NIR imaging. Based on ICG fluorescence, the blood circulation half-life of HSA-ICG-PTX ($T_{1/2} = 1.46$ h) was significantly prolonged compared to HSA-ICG ($T_{1/2} = 0.43$ h)

and free ICG. The results also showed that HSA-ICG-PTX in laser irradiation was able to induce the most effective cancer cell death (the relative survival rate of 4T1 cells was about 0.05) showing a clear synergistic effect in comparison to either HSA-ICG-PTX without laser irradiation (the relative cell viabilities was 0.6) or HSA-ICG-induced individual photothermal under NIR laser (the relative cell viabilities was 0.45) [20].

4.3. *The combination of ChT and PDT*

To overcome significant drug resistance for chemotherapy, PDT selectively destroys cells by locally irradiating cytotoxic ROS (*e.g.*, singlet oxygen) produced by a photosensitizer with an appropriate wavelength [40]. These intracellular ROS could easily damage cellular biomolecules by causing oxidative stress or by direct reaction with DNA molecules, leading to cell apoptosis [41].

The combination of PDT and ChT to kill cancer cells in one system could be realized by enhancing the local cytotoxicity of synergistic chemotherapeutic agents of PDT. For instance, Tang et al. loaded DOX molecules into mesoporous silica structure. The silica surface was then coated with a polydopamine shell to prevent DOX leakage under physiological circulation conditions (pH 7.4) and displayed a sustained release behavior under low pH conditions (pH 5.0). The HSA was conjugated to the polydopamine surface *via* the Michael addition reaction, and then photosensitizer Ce6 molecules were loaded into the internal HSA structure to achieve PDT function, which could increase biocompatibility and blood circulation time. The contents of DOX and Ce6in this nanoplatform were optimized by UV−vis spectrophotometer, and the contents were ∼22.8% and ∼9.6% (w/w), respectively. Besides, the anti-tumor effect was shown by U87 cells viability incubated with different treatment groups at various concentrations. They discovered the cell viabilities of the synergistic PDT+ChT group, PDT and ChT group were 0.3, 0.63, 0.67, respectively, when the concentration reached 800 μg/ml. Therefore, by evaluating the inhibition effect of U87 cells, the synergistic PDT+ChT group had a greater inhibition due to the sustained release of DOX under acidic conditions and red light-induced PDT compared to the groups treated with PDT alone or ChT alone. Meanwhile, this nanoplatform could be guided to the tumor area for targeted therapy through magnetic field navigation [42].

In another study reported by Chen and his collaborators, a simple method of constructing albumin-based nanoplatforms *via* drug-induced albumin assembly could achieve tumor-targeted cancer therapy with PDT/ChT combination. Two formulations were constructed using two strategies: For the first formulation, HSA-Ce6-PTX-rgd-1 was achieved by simple mixing of HSA-Ce6 (the optimized molar radio of HSA: Ce6 = 1:3), HSA-rgd (acyclic Arg-Gly-Asp, which specially binds Rvβ3-integrin), and PTX simultaneously. For the second formulation, HSA-Ce6 was first mixed with PTX to form HSA-Ce6-PTX core nanoparticles, and HSA-rgd was assembled to them in the presence of additional PTX (HSA-Ce6-PTX-rgd-2). Both FLI and MRI results demonstrated effective tumor targeting of these drug-loaded albumin-based nanoparticles in combination with rgd. The two formulations, HSA-Ce6-PTX-rgd-1 and HSA-Ce6-PTX-rgd-2, did not differ significantly in tumor targeting ability, although having different sizes (The hydrodynamic size of HSA-Ce6-PTX-rgd-2 was larger than HSA-Ce6-PTX-rgd-1). Therefore, relative viabilities of U87MG cells were investigated after being treated with different concentrations of HSA-Ce6-PTX and the above two formulations. An significant synergistic effect of the combined PDT/ChT of nanoparticle-treated cells was observed after laser irradiation, showing superior cancer cell killing efficacy compared to PDT alone (HSA-Ce6-rgd-treated (HSA-Ce6-rgd-treated (the molar radio of HSA-Ce6: unmodified HAS = 1:1) cells with light exposure) or ChT alone (nanoparticle-treated cells without light irradiation) [36].

In 3.1.1 we cite pH-/H_2O_2-responsive HSA-MnO_2-Ce6&Pt (HMCP) nanoparticles. The preparation method of MAlb NPs is not repeated here. Cell experiments showed that compared to chemotherapy alone with HMCP in dark (L−), or PDT alone with HMC under light exposure (L+), the combined treatment by HMCP (L+) offered the most effective cancer cell killing, which could be further enhanced with additional H_2O_2. Moreover, HMCP nanoparticles, the sensitive pH/H_2O_2-responsive behaviors of MnO_2, are able to simultaneously generate O_2 *in situ* by reaction with endogenous H_2O_2 inside the tumor. Therefore, HMCP together with MnO_2 to generate oxygen *in situ* from H_2O_2 appears to be a potent H_2O_2-responsive photodynamic agent, which in the meanwhile is able to deliver cis-Pt (IV) prodrugs for combined ChT and PDT.

4.4. *The combination of PTT/PDT with chemotherapy*

Combination of PTT/PDT with chemotherapy offers unique advantages over monotherapy alone. Lian at el. developed one kind of multifunctional nanoparticles for PTT/PDT with chemotherapy for the treatment of castration-resistant prostate cancer. These nanoparticles based on IR780 (a NIR dye) and docetaxel (DTX)-loaded HSA nanoplatform (HSA-IR780-DTX). The photothermal profile after being exposed to 808 nm laser irradiation (1 W/cm^2) of the nanoparticles showed that HSA-IR780 and HSA-IR780-DTX solutions exhibited the similar profiles and the temperature changes of nanoparticles were concentration dependent. The maximum temperature of HSA-IR780 and HSA-IR780-DTX (20 μg/ml) was found to be 47.5 °C. The fluorescence intensity of singlet oxygen sensor green and green fluorescence produced by oxidized H_2DCFDA gradually increased under the 808 nm laser irradiation, indicating the generation of singlet oxygen and ROS respectively. All these verified the HSA-IR780-DTX has photodynamic effects. The therapeutic efficacy of each treatment was monitored by assessing tumor volumes for 18d. It was obvious that tumor size of the laser group HSA-IR780 was similar to that of the laser group HSA-IR780-DTX within the first 3d after treatment. However, 3d later, due to the combined action of PTT and chemotherapy, HSA-IR780 with laser group gradually showed tumor regeneration, while the laser group HSA-IR780-DTX showed continuous tumor growth inhibition effect. In contrast, tumors on mice with ChT alone (HSA-DTX, HSA-IR780-DTX without laser) or with PTT alone (HSA-IR780 with laser) showed a moderate growth inhibition effect. The cell viability of cells treated with HSA-IR780-DTX plus laser irradiation (The cell viability was 0.25 at

1.5 μg/ml concentrations of IR780) was much lower than that of cells treated with other groups. The above phenomenons suggested a significantly superior combination effect compared to monotherapy. The difference from the drug release triggered by photodynamic as described above was that there were no significant differences release profiles of DTX from HSA-IR780-DTX nanocomposite with NIR laser illumination and without NIR laser illumination [43].

5. Conclusions and outlook

In summary, the present paper mainly introduces various MAlb-NPs in the past five years. The multifunctionality is reflected in the strategy of multi-mode therapy through biomedical imaging technology. Intelligence means that the nano-antitumor drug delivery system has stimuli-response characteristics. The components of MAlb-NPs, the interaction between cargo and albumin, and the way of binding were analyzed. As the so-called structures defines functions, the albumin-based nanoplatforms evolved from a simple drug-albumin complex to a variety of cargo (including drugs)-albumin complexes to realize intelligence and multifunction.

As far as we know, tumor hypoxic conditions will lead to RIT and PDT generating resistance. So it has been reported that MAlb-NPs release oxygen through the MnO_2 decomposing H_2O_2 under acidic conditions or by Cat, and then tumor hypoxia was remitted to increase photosensitizer activity and promoted drug release. However, the use of photosensitizer consumes oxygen and exacerbates the hypoxic status of the tumor, although the resulting ROS can be used to synergize with chemotherapeutic drugs. Therefore, how to adjust the oxygen pressure and ROS level in tumor region is still the focus that researchers need to consider.

Towards the above matters, some researchists have proposed the use of hypoxia activated prodrugs (HAPs) to combine with a photo sensitizer to achieve synergistic effects. Based on the ability of certain hydrophobic drugs to self-assemble with albumin to form nanocomposites, we can try to covalently modify HAPs so that they can be formed into prodrug-MnO_2-photosensitizers co-deliver nanocomplexes (HAP-MnO_2-PSs-Alb NCs) *in vitro* with albumin by a simple self-assembly approach. Compared with MAlb NPs, this complex can not only be expected to achieve the combined application of ChT and PDT, but also gradually released drugs according to the oxygen pressure and ROS level. It is assumed that these NCs decompose H_2O_2 to produce oxygen at low oxygen state while decomposing into smaller particles to promote deep penetration of tumors, and facilitate the contribution of PDT by photosensitizer. Once oxygen is consumed to cause a hypoxic state, HAP will be activated to produce a chemotherapeutic effect.

Promising strategies in MAlb NPs rely on understanding the unique physiological characteristics of tumor sites and application of interdisciplinary techniques. Solving the contradiction and imbalance in cancer treatment would bring new perspectives to the future fight against cancer and may provide new avenues for drug development of MAlb NPs drug delivery systems.

Declaration of interest

The authors declare that there is no conflicts of interest.

REFERENCES

[1] Tarhini M, Benlyamani I, Hamdani S, Agusti G, Fessi H, Greige-Gerges H, et al. Protein-based nanoparticle preparation via nanoprecipitation method. Materials (Basel) 2018;11(3):E394.
[2] Adamczyk Z, Pomorska A, Nattich-Rak M, Wytrwal-Sarna M, Bernasik A. Protein adsorption mechanisms at rough surfaces: serum albumin at a gold substrate. J Colloid Interface Sci 2018;30:631–41.
[3] Adamczyk Z, Nattich-Rak M, Dabkowska M, Kujda-Kruk M. Albumin adsorption at solid substrates: a quest for a unified approach. J Colloid Interface Sci 2018;514:769–90.
[4] Jachimska B, Tokarczyk K, Łapczyńska M, Puciul-Malinowska A, Zapotoczny S. Structure of bovine serum albumin adsorbed on silica investigated by quartz crystal microbalance. Colloid Surf A 2016;489:163–72.
[5] Kratz F. Albumin as a drug carrier: design of prodrugs, drug conjugates and nanoparticles. J Control Release 2008;132(3):171–83.
[6] Chen X, Liu L, Jiang C. Charge-reversal nanoparticles: novel targeted drug delivery carriers. Acta Pharm Sin B 2016;6(4):261–7.
[7] Ding D, Tang X, Cao X, Wu J, Yuan A, Qiao Q, et al. Novel self-assembly endows human serum albumin nanoparticles with an enhanced antitumor efficacy. AAPS PharmSciTech 2014;15(1):212–22.
[8] Aslan B, Ozpolat B, Sood AK, Lopez-Berestein G. Nanotechnology in cancer therapy. J Drug Target 2013;21(10):904–13.
[9] Sun B, Luo C, Cui W, Sun J, He Z. Chemotherapy agent-unsaturated fatty acid prodrugs and prodrug-nanoplatforms for cancer chemotherapy. J Control Release 2017;264:145–59.
[10] Han H, Wang J, Chen T, Yin L, Jin Q, Ji J. Enzyme-sensitive gemcitabine conjugated albumin nanoparticles as a versatile theranostic nanoplatform for pancreatic cancer treatment. J Colloid Interface Sci 2017;507:217–24.
[11] Zhang M, Zhang L, Chen Y, Li L, Su Z, Wang C. Precise synthesis of unique polydopamine/mesoporous calcium phosphate hollow Janus nanoparticles for imaging-guided chemo-photothermal synergistic therapy. Chem Sci 2017;8(12):8067–77.
[12] Liang X, Li X, Jing L, Yue X, Dai Z. Theranostic porphyrin dyad nanoparticles for magnetic resonance imaging guided photodynamic therapy. Biomaterials 2014;35(24):6379–88.
[13] Ma Y, Tong S, Bao G, Gao C, Dai Z. Indocyanine green loaded SPIO nanoparticles with phospholipid-PEG coating for dual-modal imaging and photothermal therapy. Biomaterials 2013;34(31):7706–14.
[14] Wang LV, Hu S. Photoacoustic tomography: *in vivo* imaging from organelles to organs. Science 2012;335(6075):1458–62.
[15] Hainfeld JF, Slatkin DN, Focella TM, Smilowitz HM. Gold nanoparticles: a new X-ray contrast agent. Br J Radiol 2006;79(939):248–53.
[16] Xi D, Dong S, Meng X, Lu Q, Meng L, Ye J. Gold nanoparticles as computerized tomography (CT) contrast agents. RSC Adv 2012;2(33):12515.
[17] Cheng L, Liu J, Gu X, et al. PEGylated WS(2) nanosheets as a multifunctional theranostic agent for *in vivo* dual-modal CT/photoacoustic imaging guided photothermal therapy. Adv Mater 2014;26(12):1886–93.

[18] Zhao PF, Yin WM, Wu AH, Tang YS, Wang JY, Pan ZZ, et al. Dual-targeting to cancer cells and M2 macrophages via biomimetic delivery of mannosylated albumin nanoparticles for drug-resistant cancer therapy. Adv Funct Mater 2017;27(44):1700403.
[19] Zheng MB, Zhao PF, Luo ZY, Gong P, Zheng CF, Zhang PF, et al. Robust ICG theranostic nanoparticles for folate targeted cancer imaging and highly effective photothermal therapy. ACS Appl Mater Interfaces 2014;6(9):6709–16.
[20] Chen Q, Liang C, Wang C, Liu Z. An imagable and photothermal "Abraxane-like" nanodrug for combination cancer therapy to treat subcutaneous and metastatic breast tumors. Adv Mater 2015;27(5):903–10.
[21] Burger AM, Hartung G, Stehle G, Sinn H, Fiebig HH. Pre-clinical evaluation of a methotrexate-albumin conjugate (MTX-HSA) in human tumor xenografts *in vivo*. Int J Cancer 2001;92(5):718–24.
[22] Mocanu MN, Yan F. Ultrasound-assisted interaction between chlorin-e6 and human serum albumin: pH dependence, singlet oxygen production, and formulation effect. Spectrochim Acta A Mol Biomol Spectrosc 2018;190:208–14.
[23] Kratz F, Warnecke A, Scheuermann K, et al. Probing the cysteine-34 position of endogenous serum albumin with thiol binding doxorubicin derivatives. J Med Chem 2002;45:5523–33.
[24] Zheng K, Setyawati MI, Leong DT, Xie J. Antimicrobial gold nanoclusters. ACS Nano 2017;11(7):6904–10.
[25] Chen J, Chen Q, Liang C, Yang Z, Zhang L, Yi X, et al. Albumin-templated biomineralizing growth of composite nanoparticles as smart nano-theranostics for enhanced radiotherapy of tumors. Nanoscale 2017;9(39):14826–35.
[26] Chen Y, Ye D, Wu M, Chen H, Zhang L, Shi J, et al. Break-up of two-dimensional MnO_2 nanosheets promotes ultrasensitive pH-triggered theranostics of cancer. Adv Mater 2014;26(41):7019–26.
[27] Tao WH, He ZG. ROS-responsive drug delivery systems for biomedical applications. Asian J Pharm Sci 2018;13(2):101–12.
[28] He X, Li J, An S, Jiang C. pH-sensitive drug-delivery systems for tumor targeting. Ther Deliv 2013;4(12):1499–510.
[29] Chen Q, Feng LZ, Liu JJ, Zhu WW, Dong ZL, Wu YF, et al. Intelligent albumin-MnO_2 nanoparticles as pH-/H_2O_2-responsive dissociable nanocarriers to modulate tumor hypoxia for effective combination therapy. Adv Mater 2016;28(33):7129–36.
[30] Tian L, Chen Q, Yi X, Chen J, Liang C, Chao Y, et al. Albumin-templated manganese dioxide nanoparticles for enhanced radioisotope therapy. Small 2017;13(25):1700640.
[31] Cheetham AG, Zhang P, Lin YA, Lock LL, Cui H. Supramolecular nanostructures formed by anticancer drug assembly. J Am Chem Soc 2013;135(8):2907–10.
[32] Sheng ZH, Hu DH, Zheng MB, Zhao PF, Liu HL, Gao DY, et al. Smart human serum albumin-indocyanine green nanoparticles generated by programmed assembly for dual-modal imaging-guided cancer synergistic phototherapy. ACS Nano 2014;8(12):12310–22.
[33] Wang J, Mao W, Lock LL, Tang J, Sui M, Sun W, et al. The role of micelle size in tumor accumulation, penetration, and treatment. ACS Nano 2015;9:7195–206.
[34] Cheng Q, Chen JW, Liang C, Feng LZ, Dong ZL, Song XJ, et al. Drug-induced co-assembly of albumin/catalase as smart nano-theranostics for deep intra-tumoral penetration, hypoxia relieve, and synergistic combination therapy. J Control Release 2017;263:79–89.
[35] Peralta DV, Heidari Z, Dash S, Tarr MA. Hybrid paclitaxel and gold nanorod-loaded human serum albumin nanoparticles for simultaneous chemotherapeutic and photothermal therapy on 4T1 breast cancer cells. ACS Appl Mater Interfaces 2015;7(13):7101–11.
[36] Chen Q, Wang X, Wang C, Feng L, Li Y, Liu Z. Drug-induced self-assembly of modified albumins as nano-theranostics for tumor-targeted combination therapy. ACS Nano 2015;9(5):5223–33.
[37] Karantanos T, Corn PG, Thompson TC. Prostate cancer progression after androgen deprivation therapy: mechanisms of castrate resistance and novel therapeutic approaches. Oncogene 2013;32(49):5501–11.
[38] Sasidharan S, Bahadur D, Srivastava R. Protein-poly(amino acid) nanocore-shell mediated synthesis of branched gold nanostructures for CT imaging and photothermal therapy of cancer. ACS Appl Mater Interfaces 2016;8(25):15889–903.
[39] Hou W, Xia F, Alfranca G, et al. Nanoparticles for multi-modality cancer diagnosis: simple protocol for self-assembly of gold nanoclusters mediated by gadolinium ions. Biomaterials 2017;120:103–14.
[40] Park YI, Kim HM, Kim JH, Moon KC, Yoo BJ, Lee KT, et al. Theranostic probe based on lanthanide-doped nanoparticles for simultaneous *in vivo* dual-modal imaging and photodynamic therapy. Adv Mater 2012;24(42):5755–61.
[41] Zhang Y, Huang F, Ren C, Yang L, Liu L, Cheng Z, et al. Targeted chemo-photodynamic combination platform based on the DOX prodrug nanoparticles for enhanced cancer therapy. ACS Appl Mater Interfaces 2017;9(15):13016–28.
[42] Tang XL, Jing F, Lin BL, Cui S, Yu RT, Shen XD, et al. pH-responsive magnetic mesoporous silica-based nanoplatform for synergistic photodynamic therapy/chemotherapy. ACS Appl Mater Interfaces 2018;10(17):15001–11.
[43] Lian HB, Wu JH, Hu YQ, Guo HQ. Self-assembled albumin nanoparticles for combination therapy in prostate cancer. Int J Nanomed 2017;12:7777–87.
[44] Holbrook RJ, Rammohan N, Rotz MW, MacRenaris KW, Preslar AT, Meade TJ. Gd(III)- dithiolane gold nanoparticles for T1-weighted magnetic resonance imaging of the pancreas. Nano Lett 2016;16(5):3202–9.
[45] Zhang H, Wang T, Zheng Y, Yan C, Gu W, Ye L. Comparative toxicity and contrast enhancing assessments of Gd_2O_3@BSA and MnO_2@BSA nanoparticles for MR imaging of brain glioma. Biochem Biophys Res Commun 2018;499(3):488–92.
[46] Jeon S, Oberreit DR, Van Schooneveld G, Gao Z, Bischof JC, Haynes CL, et al. Ion mobility based quantification of surface coating dependent binding of serum albumin to superparamagnetic iron oxide nanoparticles. ACS Appl Mater Interfaces 2016;8(37):24482–90.
[47] Kostiv U, Lobaz V, Kučka J, Švec P, Sedláček O, Hrubý M, et al. A simple neridronate-based surface coating strategy for upconversion nanoparticles: highly colloidally sTable 125I-radiolabeled $NaYF_4$:yb^{3+}/Er^{3+}@PEG nanoparticles for multimodal *in vivo* tissue imaging. Nanoscale 2017;9(43):16680–8.
[48] Huang H, Yang DP, Liu M, Wang X, Zhang Z, Zhou G, et al. pH-sensitive Au-BSA-DOX-FA nanocomposites for combined CT imaging and targeted drug delivery. Int J Nanomed 2017;12:2829–43.
[49] Wang Q, Kuo Y, Wang Y, Shin G, Ruengruglikit C, Huang Q. Luminescent properties of water-soluble denatured bovine serum albumin-coated CdTe quantum dots. J Phys Chem B 2006;110(34):16860–6.

[50] You Q, Sun Q, Yu M, Wang J, Wang S, Liu L, et al. BSA-bioinspired gadolinium hybrids functionalized hollow gold nanoshells for NIRF/PA/CT/MR quad-modal diagnostic imaging guided photothermal/photodynamic cancer therapy. ACS Appl Mater Interfaces 2017;9(46):40017–30.
[51] Chen Q, Liu X, Zeng J, Cheng Z, Liu Z. Albumin-NIR dye self-assembled nanoparticles for photoacoustic pH imaging and pH-responsive photothermal therapy effective for large tumors. Biomaterials 2016;98:23–30.
[52] Gao FP, Cai PJ, Yang WZ, Xue JQ, Gao L, Liu R, et al. Ultrasmall [64Cu]Cu nanoclusters for targeting orthotopic lung tumors using accurate positron emission tomography imaging. ACS Nano 2015;9(5):4976–86.
[53] Lee SP, Im HJ, Kang S, Chung SJ, Cho YS, Kang H, et al. Noninvasive imaging of myocardial inflammation in myocarditis using 68Ga-tagged mannosylated human serum albumin positron emission tomography. Theranostics 2017;7(2):413–24.
[54] Xu R, Fisher M, Juliano RL. Targeted albumin-based nanoparticles for delivery of amphipathic drugs. Bioconjug Chem 2011;22(5):870–8.
[55] Abbasi S, Paul A, Shao W, Prakash S. Cationic albumin nanoparticles for enhanced drug delivery to treat breast cancer: preparation and *in vitro* assessment. J Drug Deliv 2012;2012:686108.
[56] Lin T, Zhao P, Jiang Y, Tang YS, Jin HY, Pan ZZ, et al. Blood–brain-barrier-penetrating albumin nanoparticles for biomimetic drug delivery via albumin-binding protein pathways for antiglioma therapy. ACS Nano 2016;10(11):9999–10012.
[57] Yu XZ, Zhu W, Di Y, Gu J, Guo Z, Li H, et al. Triple-functional albumin-based nanoparticles for combined chemotherapy and photodynamic therapy of pancreatic cancer with lymphatic metastases. Int J Nanomed 2017;12:6771–85.
[58] Wang D, Meng L, Fei Z, Hou C, Long J, Zeng L, et al. Multi-layered tumor-targeting photothermal-doxorubicin releasing nanotubes eradicate tumors *in vivo* with negligible systemic toxicity. Nanoscale 2018;10:8536–46.